Effects of tensile and compressive in-plane stress fields on adhesion in laser induced delamination experiments

Fedorov, A.; Vellinga, W. P.; de Hosson, J. Th. M.

Published in:
Journal of Applied Physics

DOI:
10.1063/1.2925796

Effects of tensile and compressive in-plane stress fields on adhesion in laser induced delamination experiments

A. Fedorov, W. P. Vellinga, and J. Th. M. De Hosson[a)]
Department of Applied Physics, The Netherlands Institute for Metals Research and Zernike Institute for Advanced Materials, University of Groningen, Nijenborgh 4, 9747 AG Groningen, The Netherlands

(Received 28 October 2007; accepted 14 March 2008; published online 23 May 2008)

In this work, the adhesion of a polymer coating on steel substrate subjected to uniaxial tensile plastic deformations was studied with the laser induced delamination technique. A decrease in the practical work of adhesion has been measured as the deformation of the substrate progressed. Moreover, it was observed that the deformation of the metal substrate introduced in-plane stresses in the polymer coating. Delamination was studied under compressive or tensile in-plane stresses. The model presented enabled to derive from the experimental data not only the practical work of adhesion but also the magnitude and the character (tensile or compressive) of the in-plane stress. The strain fields of the metal substrate during plastic deformation and after the elastic relaxation were monitored with a digital image correlation analysis system. The measured strain fields were confronted to the in-plane stresses obtained from the delamination experiments. © *2008 American Institute of Physics*. [DOI: 10.1063/1.2925796]

I. INTRODUCTION

In modern automotive and packaging industries, polymer precoated metal sheets are subjected to significant plastic deformations during shape forming steps such as stamping or draw-redraw processing.[1] To predict the integrity of the polymer-metal interfaces, one requires a reliable method to monitor the adhesion of the interface before and after the deformations. Quantitative characterization of adhesion of polymer-metal interfaces subjected to deformation is complicated by the presence of residual in-plane stresses introduced during processing. In an adhesion test of a deformed specimen, delamination takes place under a combination of the pre-existing residual stresses and the stress fields applied by external loading.[2–4] In some instances, residual stresses alone can lead to a spontaneous delamination or buckling. Accurate accounting for the residual stresses is essential if one aims at understanding the physical and chemical mechanisms of adhesion in the deformed polymer-metal interfaces.

Residual stresses can be introduced by a mechanical deformation, a deposition process, or by a mismatch in thermal expansion coefficient between the coating and the substrate. Blister tests, both pressurized and shaft loaded in the presence of in-plane residual stresses were considered by Jensen and Thouless.[5] Williams presented the analysis of the energy release rate for a number of adhesion testing geometries with tensile residual stress.[6] Guo *et al.* showed that uniform tensile residual stresses reduce central deflection in the blister test under small loads when bending is dominant.[7] Bouchet *et al.*[8] and Guo *et al.*[4] considered the effect of residual stresses on the strain energy release rate measured with a double cantilever adhesion test. Daghyani *et al.* studied the effect of thermal residual stress on the local crack-tip stress field and the path of crack propagation.[9] Gay has studied the adhesion properties of rubber, which was stressed prior to the adhesion test.[10] The decrease in adhesion of the stretched rubber was ascribed to the changes in mechanical properties of the rubber rather than to changes in the surface energy. Vayede and Wang studied the adhesion of polymer coating of metal sheet under plastic deformation.[11] Cross-cut tape test was used to evaluate the performance of the coating in terms of the so-called forming limit diagram, which was used in sheet metal forming. Litteken *et al.* investigated the effect of thermal residual stress on the contribution from plastic dissipation to interfacial fracture energy.[12] The compressive residual stress in the ductile layer was found to enhance plasticity and, therefore, fracture resistance, while tensile stresses reduce plasticity and fracture resistance.

In this work, adhesion of polymer-metal interface is characterized with the laser induced delamination technique. The detailed description of this method can be found in Refs. 13 and 14. In this method, pressurized cylindrically shaped blisters are formed at the interface with an infrared pulsed laser. Under the pressure created inside the blisters, polymer coating delaminates further until the corresponding delamination energy release rate equals to the practical work of adhesion. From the shape of the blister, the related stress fields and the practical work of adhesion are derived.[14]

A substantial amount of works on modeling of the classical blister test can be found in literature.[5–7,13,15] However, there are a number of principle differences between the classical blister test and the one presented in this work. Most models describe spherical blisters, while in the laser induced delamination, a cylindrical symmetry is used. In the classical blister test, the blister pressure is constant during the delamination. In the laser induced delamination, the amount of gas generated inside the blister is constant but the pressure drops when the delamination takes place. As a consequence, in both cases, different expressions for the energy release rate are obtained. Another significant difference is that the over-

[a)]Author to whom correspondence should be addressed. Electronic mail: j.t.m.de.hosson@rug.nl.

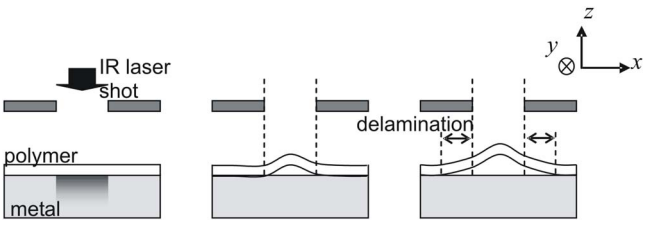

FIG. 1. (Color online) Schematic presentation of the laser induced delamination technique. A series of subsequent laser shots is performed through the slit. After the blister is formed, delamination of the coating can proceed further provided that the energy release rate exceeds the practical work of adhesion.

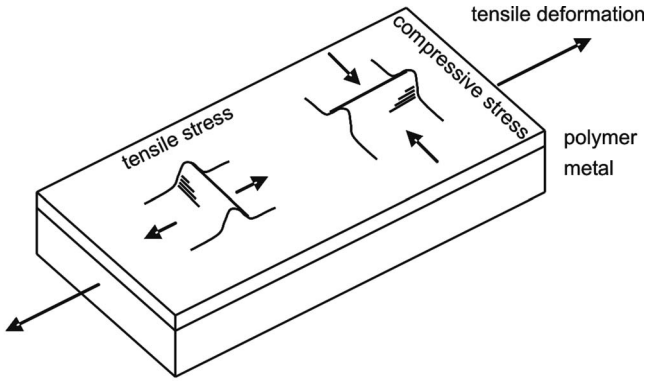

FIG. 2. Geometry of the experiments. Blisters formed perpendicular to the axis of deformation experience tensile in-plane stress. Blisters formed parallel to the axis of deformation experience compressive in-plane stress.

pressure inside the laser produced blister is not very high; therefore, the effect of the atmospheric pressure should be accounted. As a consequence, the experimental data are analyzed by using the elastic model and with the finite element analysis developed by the authors, as presented in Refs. 14 and 16. The improved version of this model, which accounts for the stretching of the midplane of the polymer film, is reported in this paper.

The experimental results present the adhesion measurements performed on steel samples with a polyethylene terephthalate (PET) coating, which were subjected to a uniaxial plastic deformation. Remarkable is that depending on the orientation of the blisters with respect to the axis of deformation, delamination under compressive or tensile in-plane stresses was studied on the same sample. From the analysis of the blister shape, the in-plane stresses and the practical work of adhesion are derived.

II. EXPERIMENTAL

In this work, adhesion of the polymer on steel was measured by means of the laser induced delamination technique, which is schematically presented in Fig. 1. In this method, a coating under study is subjected to a series of laser pulses with stepwise increase in intensity. Every shot is carried out through a slit which results in a formation of a cylindrically shaped blister. Such geometry is chosen for two reasons. First, to enable the description of the formation of the blisters with a two dimensional (2D) simple elastic model.[14] Second, different from the case of circular blisters, the profile measurements of a cylindrical blister are not very sensitive to the exact path, along which the profile is measured. Upon increasing the laser pulse intensity, the pressure inside the blister reaches the critical value, which results in a further delamination of the coating. The blister profiles are measured with the stylus profiler and by applying the elastic model, the stress fields inside the coating and the practical work of adhesion are derived.

The blisters were produced with the infrared Nd:YAG (yttrium aluminum garnet) laser NL303HT from EXPLA with the maximum pulse energy of 800 mJ and 5 ns pulse duration. The blister profiles were measured with the stylus Perthometer S2 from Mahr. The samples under study were obtained from CORUS and present a 30 μm layer of PET on interstitial free steel substrate with a thickness of 240 μm.

In previously presented experiments, the slit opening, which defines the initial width of the blisters, was preserved through the whole series of measurements.[14] As the laser power increases, the initial overpressure generated inside the blisters rises as well. Consequently, at every new step, the delamination starts with higher values of the energy release rate. The delamination proceeds under the condition that the energy release rate exceeds the certain value, which is defined as the practical work of adhesion. The amount of gas inside the blister is fixed and, therefore, the overpressure and the energy release rate decrease during the delamination until the mentioned criterion is not fulfilled and the delamination stops. In order to keep the delamination process close to the thermodynamic equilibrium, the initial value of the energy release rate should be just above the measured value of the practical work of adhesion. This is achieved by increasing the opening of the slit with the laser power. This new approach, which is used in the presented measurements, has considerably improved the agreement between the model and the experiment.

To study the effect of deformation on adhesion, the samples were uniaxially stretched in the material testing system MTS 810. Both bonelike and rectangular shapes of the samples were used with no measurable difference. The sample dimensions were of 25×75 mm^2. The samples were clamped at the edges leaving an area of approximately 20×40 mm^2 with uniform deformation for the adhesion measurements. The metal substrate was plastically deformed under nearly plane stress condition, with the strain values ranging from 0.3% to 2.0%. In the direction perpendicular to the deformation, the dimension of the substrate reduced. By using the digital-image correlation noncontact optical three dimensional (3D) deformation measuring system (Aramis), the strain fields of the metal substrate during the plastic deformation and after the elastic relaxation (less than 0.1%) were recorded. After the samples were removed from the MTS testing system, the polymer coating remained under in-plane stresses because of the plastic deformation of the substrate. In the direction of deformation, the stress was tensile and in the perpendicular direction, the stress was compressive. By using the same sample and choosing the orientation of the blisters parallel or perpendicular to the axis of deformation, as shown in Fig. 2, the delamination of the coating was studied in the presence of compressive or tensile in-plane stresses.

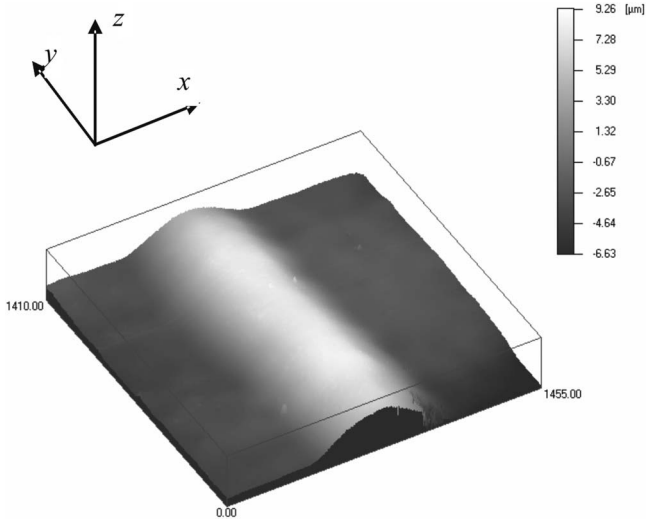

FIG. 3. Blister shape observed with the confocal microscope. Directions of the axis used in the model are indicated.

III. FITTING MODEL

The objective of the fitting procedure is to obtain the practical work of adhesion and the in-plane stress present in the coating from the shape of a blister. To do that, one has to be able to derive the elastic energy stored in the blister wall and the energy of the gas pressurized inside the blister. The energy changes (global energy release rate) during the delamination will then be related to the practical work of adhesion.

A cylindrical blister aligned along the y axis can be described as a thin plate clamped along the boundaries parallel to the y axis. (The orientation of the axis is given in the insets in Figs. 1 and 3). The governing equation for the deflection w of the plate under normal uniform pressure p and in presence of the midplane stress σ_{mp} is written as[17]

$$\frac{d^4w}{dx^4} = \frac{p}{D} - \frac{\sigma_{mp}t}{D}\frac{d^2w}{dx^2}. \tag{1}$$

$D=Et^3/12(1-\nu^2)$ is the flexural rigidity, E is the modulus of elasticity, ν is Poisson's ratio, and t is the film thickness. The midplane stress σ_{mp} is negative if compressive and is positive if tensile. Clamped or built-in, boundary conditions are used

$$w = 0, \quad w' = 0 \quad \text{at } x = -\frac{a}{2} \text{ and } x = \frac{a}{2}, \tag{2}$$

where a is the dimension of the blister along the x axis (blister width).

We presented the analytic solutions of the boundary value problems (1) and (2) without the midplane stress and with the constant compressive midplane stress σ_{mp} in Ref. 18. In this work, a numerical approach is used which enables us to account for the stretching of the midplane during blister formation. The midplane strain (in the x direction) comprises of two parts,

$$\varepsilon_{mp} = \varepsilon^0_{mp} + \tfrac{1}{2}(w')^2. \tag{3}$$

The first term corresponds to the midplane strain under the initial midplane stress σ^0_{mp}. The second term is strictly positive and represents the stretching of the midplane because of the bending of the film. Thus, the midplane stress σ_{mp} present in Eq. (1) is no longer a constant and becomes a function of x,

$$\sigma_{mp} = \sigma^0_{mp} + \frac{1}{2}\frac{E}{1-\nu^2}(w')^2. \tag{4}$$

Consider delamination of a blister during which the width of a blister changes from a_1 to $a_2=a_1+\Delta a$. The amount of gas inside the blister M is assumed to be constant. By solving the boundary value problems (1) and (2) under the condition $(p_{atm}+p)V=M$, the corresponding values of the blister pressures p_1 and p_2 are found. V is the blister volume per unit length: $V=\int_{-a/2}^{a/2} w dx$ and p_{atm} is the atmospheric pressure. The energy release rate upon delamination has contributions of the following causes:

(1) Helmholtz free energy per unit length: $\Delta F=-(p_{atm}+p_1)(V_2-V_1)$

(2) bending energy per unit length: $\Delta U_b=U_b(2)-U_b(1)$, where

$$U_b = \frac{D}{2}\int_{-a/2}^{a/2} (w'')^2 dx, \tag{5}$$

and (3) midplane stretching or/and compression energy per unit length $\Delta U_{mp}=U_{mp}(2)-U_{mp}(1)$, where

$$U_{mp} = \frac{h}{2}\int_{-a/2}^{a/2} \sigma_{mp}\varepsilon_{mp} dx. \tag{6}$$

The energy balance should also include the strain energy of a small fraction of the coating with the width of Δa, which after the delamination is incorporated within the blister wall

$$\delta U_{\Delta a} = \frac{\Delta a t}{2}\frac{(1-\nu^2)}{E}(\sigma^0_{mp})^2. \tag{7}$$

The released energy is spent on delamination Gda and on the work against the atmospheric pressure $\delta A=p_{atm}\Delta V$ (per unit length). G is the practical work of adhesion in the usual units of J/m^2. In the experiments, the blister profiles are measured when the delamination process has already stopped. Therefore, the energy characteristics obtained from the blister shape correspond to the condition when the energy release rate is equal to the practical work of adhesion. Per unit length, this condition is written in the following way:

$$p\Delta V - (\Delta U_b + \Delta U_{mp} - \delta U_{\Delta a}) = G\Delta a. \tag{8}$$

Every blister profile is characterized by two parameters: blister height H and blister width a. Therefore, a series of measured profiles generates a set of experimental data: $\{H_i, a_i\}$. To derive the midplane stress σ_{mp} and the work of adhesion G from the experimental data, one has to provide a fitting function, for example, $H=H(a;G,\sigma_{mp})$, where G and σ_{mp} are the fitting parameters. However, the equations discussed above do not offer a simple expression for the blister height expressed as a function of a, G, and σ_{mp}. Instead, one has to

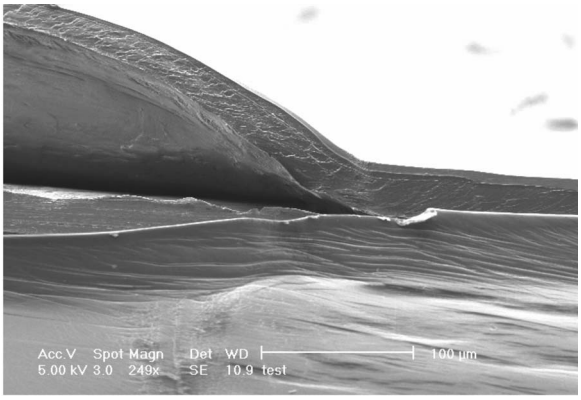

FIG. 4. SEM image with the opening of the blister with no signs of plastic deformation.

fix the amount of gas inside the blister M and to follow the delamination process by increasing stepwise the blister width. At every step, $a=a_k$, the blister height and the energy release rate, which is equal to the practical work of adhesion, are calculated. Such procedure will result in a set of values $\{H_k, G_k\}$. By repeating this operation for a set of different values of the midplane stress $\sigma_{\mathrm{mp}}=\sigma_m$, one can construct a 3D table of $H_{k,l,m}$ defined on the mesh $\{a_k, G_l, \sigma_m\}$. Consequently, the fitting function $H=H(a;G,\sigma_{mp})$ is obtained by using a 3D spline and the constructed table. Eventually, to perform the fit $H=H(a_i;G,\sigma_{mp})\rightarrow H_i$, the nonlinear iterative Levenberg–Marquardt algorithm is used.[19]

IV. RESULTS AND DISCUSSION

A typical blister observed in confocal microscope is shown in Fig. 3. Note that the vertical axis has a different scale. Usually, the blister height does not exceed 30 μm, while the blister width is about 1 mm. One of the main objectives of any adhesion measuring techniques is to produce as little plastic deformation in the coating during delamination as possible. It has been argued earlier[14] that with the laser induced delamination technique, the introduced plastic deformation is minimized and mostly restricted to the near crack-tip area. One reason is that the delamination takes place very fast leaving no time for plastic relaxations of the coating. Second, the stress fields developed in the bulk of the polymer film do not exceed the elastic regime of PET, of about 50–60 MPa. Indeed, in the scanning electron microcopy (SEM) image of the blister opening presented in Fig. 4, no signs of plastic deformation of the blister wall or crazing are observed. The area of the blister wall presented in the image was not exposed to the laser radiation and the opening is formed via delamination of the coating under the gas pressure.

The results of the laser induced delamination experiments performed on undeformed reference sample are shown in Fig. 5. Every symbol represents the dimensions of the blister, height and width, which is formed at certain level of the laser power. The contour lines on this graph present the lines of constant work of adhesion measured in J/m^2 and calculated by the procedure presented in Sec. III or with a simple analytic expression derived earlier[14]

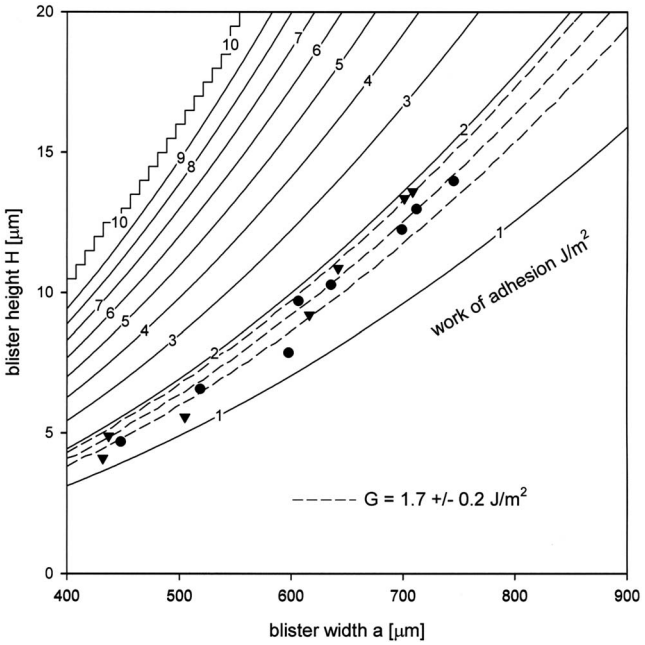

FIG. 5. Blister dimension, height vs width, obtained in two series of measurements performed on an undeformed sample. The contour lines are defined by Eq. (9) and represent the lines of constant work of adhesion.

$$G = 512D\frac{H^2}{a^4}. \tag{9}$$

Two sets of data present the measurements of the blisters formed in parallel and in perpendicular to the axis of deformation direction. The results show no difference in the orientation of the blisters and the data points follow the same contour line with the practical work of adhesion of $G=1.7$ J/m^2. The flexural rigidity D is calculated for the PET film thickness of $t=30$ μm, with Young's moduli of $E=2$ GPa and Poisson's ratio of $\nu=0.35$.[20]

Steel samples with a PET coating were subjected to uniaxial tensile deformation ranging from 0.3% to 2%. The steel substrate is plastically deformed so that after removing the samples from the testing machine, the coating still experiences in-plane stresses. The deformation of the substrate is under nearly plane stress condition, thus in the perpendicular direction, the size of the samples decreases. Because of much lower values, Young's moduli and the yield strength, the coating is elastically deformed. As shown in Fig. 2, if the blister orientation is perpendicular to the axis of deformation, the delamination of the coating proceeds under a tensile in-plane stress. If the orientation of the blisters is parallel to the axis of deformation, it could be argued whether one can expect compressive or tensile in-plane stress. Poisson's ratio for PET is usually claimed to be 0.35–0.45.[20] Thus, if the shrinking of the substrate exceeds this value, the in-plane stress is expected to be compressive. Otherwise, the in-plane stress in the coating is tensile in both directions. As will be shown below, in the current experiments, the coating experienced compressive in-plane stress in the direction perpendicular to the axis of deformation. That was first concluded from the laser induced delamination experiments and then was directly proved with the Aramis deformation measuring

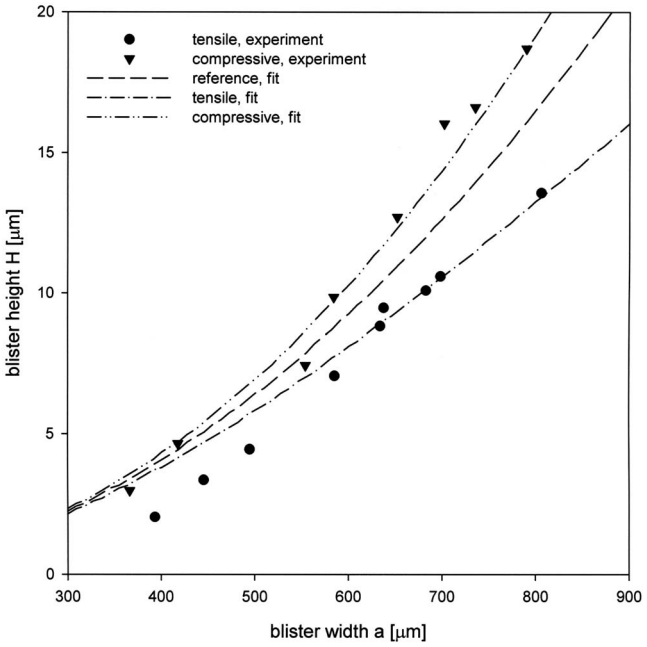

FIG. 6. Blister dimension, height vs width, obtained in two series of measurements performed on a deformed sample ($\varepsilon=1.0\%$). In one series, the blisters are formed perpendicular to the axis of deformation (circles) and in the other series the blisters are formed parallel to the axis of deformation (triangles). Dash lines present the fit.

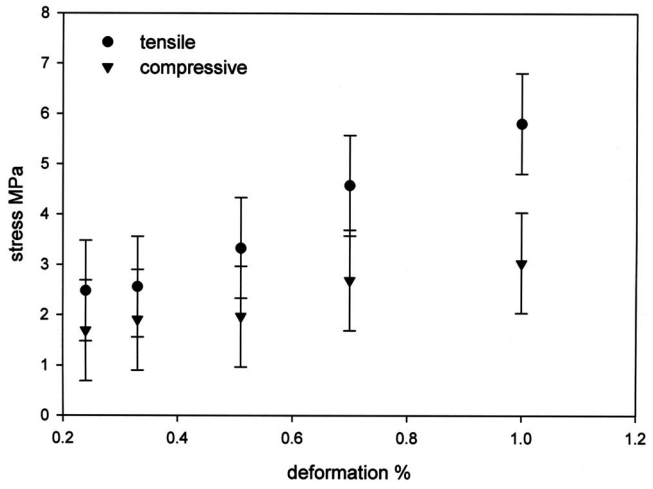

FIG. 7. In-plane tensile and compressive stresses present in the coating of deformed samples, as obtained from the fit of the blister profiles.

system. This finding is very fortunate because both tensile and compressive in-plane stress conditions can be observed on the same sample.

In contrast to the reference sample, blister parameters measured on the deformed sample do demonstrate a strong dependency on the orientation of the blisters with respect to the axis of deformation. That is shown in Fig. 6. The blisters formed under the condition of compressive in-plane stress appear to be higher than the blisters created on the reference sample with the same laser power. Tensile in-plane stress produces the opposite effect. That happens because the in-plane stress has a nonzero vertical projection if the coating is bended. The second term in the right-hand part of Eq. (1) exactly presents the product of the in-plane stress σ_{mp} and the bending curvature of the coating $\chi=-w''$. If the stress is compressive, i.e., $\sigma_{\mathrm{mp}}<0$, this term adds up with the blister pressure, which results in higher blisters. If the stress is tensile, the second term is negative and the effect of the gas pressure is reduced resulting in lower blisters.

It was assumed that the practical work of adhesion is the characteristic of the metal-polymer interface and is not significantly affected by the in-plane stresses present in the bulk of the polymer coating. Therefore, both sets of data were fitted with only three fitting parameters: G, $\sigma_{\parallel}$, and $\sigma_{\perp}$, where parameters $\sigma_{\parallel}$ and $\sigma_{\perp}$ are referred to the direction of the stress with respect to the axis of deformation, parallel or perpendicular. The results of the fits are shown with the broken lines. The results for the reference sample are also given for the sake of comparison. The contour lines are removed because for every in-plane stress, they are different.

The fitting procedure was carried out for all deformed samples. Although no initial assumption has been made about the sign of the in-plane stresses $\sigma_{\parallel}$ and $\sigma_{\perp}$, in all of the cases, $\sigma_{\parallel}$ appeared to be tensile and $\sigma_{\perp}$ appeared to be compressive. The results of the fit are summarized in Fig. 7 and 8. In Fig. 7, the absolute values of the in-plane stresses are plotted versus the deformation of the substrate. The uncertainties of the fitting parameters ΔG and $\Delta\sigma$ are taken such that about 70% of the data points in every series of measurements are bounded between two curves $H(a;G+\Delta G,\sigma-\Delta\sigma)$ and $H(a;G-\Delta G,\sigma+\Delta\sigma)$, as shown in Fig. 5. Every point is represented as 2D Gaussian with the $\Delta H=0.05$ μm and $\Delta a=0.01$ mm. This approach provides an estimate of $\Delta G\leq 0.2$ J/m^2 and $\Delta\sigma\leq 1$ MPa. As a matter of course, as the deformation progresses, the absolute values of the in-plane stress increase. For all of the samples, the compressive stress is about half of the value of the tensile.

In order to measure the actual strain fields of the metal substrate during the plastic deformation and after the elastic relaxation, the Aramis noncontact optical 3D deformation measuring system was used. The back side of the sample, which was not laminated, was sprayed with black paint to create a stochastic pattern. Based on the correlations between local displacements of the pattern elements during deformation, the Aramis system evaluates the actual displacements and the strain fields at the surface of the sample. The results of such measurements for one of the deformed sample are presented in Fig. 9. The contour plots present the values of the two principal strains. The directions of the principal strains are not shown because in every location of the sample, the tensile principal strain is parallel to the axis of deformation and the compressive strain is perpendicular to this direction. Both images show reasonable homogeneity of the strain fields, especially in the area indicated by the dash line, where the laser induced delamination experiments were performed. The measured tensile strain appeared to be lower than what was expected. This sample was deformed at 1.5% while only 1.2% of strain was measured. The compressive strain is about half the value of the tensile, which is in agreement with the typical ratio between the corresponding in-plane stresses measured in the delamination experiments. The principal strains measured for all samples are presented in Table I. The table also contains columns representing the

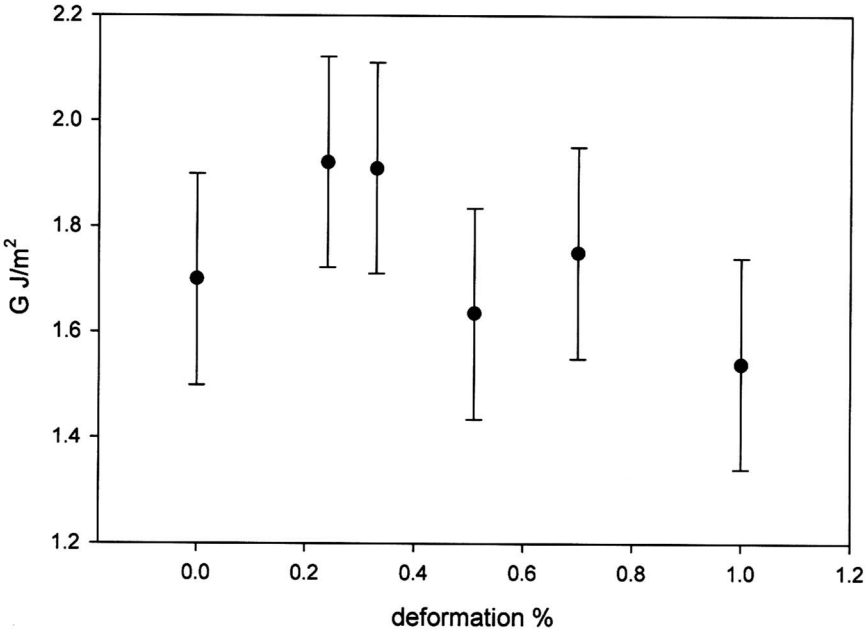

FIG. 8. Practical work of adhesion measured on the deformed samples.

in-plane stresses derived from the delamination experiments, carried out however on different samples. The agreement between these two kinds of measurements is only by the order of magnitude, considering that Young's modulus of PET is 2–3 GPa.[20]

The practical work of adhesion measured on the deformed samples with the laser induced delamination technique are presented in Fig. 9. The work of adhesion gradually decreases as the deformation of the substrate progresses. It appears that the work of adhesion measured on the reference sample is lower than those measured on some of the deformed samples. The reference measurements were performed on the samples prepared from a different laminated metal sheet. That, together with the different optical arrangements of the setup used and the inhomogeneity of the laser beam, could introduce some systematic error. Since the in-plane stresses introduced by the deformation has been already accounted, this degradation of adhesion is exclusively related to the changes that take place at the polymer-metal interface. Various physical mechanisms can be held responsible for the measured degradation of adhesion: change in the contact area, increase in the substrate roughness, breaking of the oxide layer between the substrate and the coating, etc. In future, these mechanisms will be considered in greater detail. In this work, only the roughness of the substrate was measured. However, the substrate of undeformed samples already showed a significant roughness with rms=0.35 μm. The roughness of the deformed samples has slightly increased up to rms=0.4 μm. Therefore, there are no any conclusions on correlation between the measured practical work of adhesion and substrate roughness in this study.

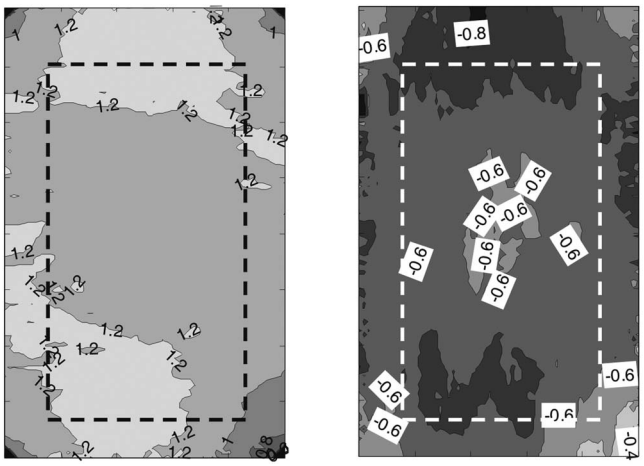

FIG. 9. Principle strain fields measured by the Aramis system. In the figure, the samples are deformed in vertical direction. Left: tensile strain parallel to the deformation axis. Right: compressive strain perpendicular to the deformation axis.

V. CONCLUSIONS

The PET coatings on steel substrate were subjected to a uniaxial tensile deformation. The adhesion of the polymer-metal interface was monitored with the laser induced delamination technique. As the deformation of the substrate increased, the degradation of adhesion in terms of the practical work of adhesion was measured. The deformation of the substrate also introduced in-plane stresses in the coating. De-

TABLE I. The in-plane principle strains $\varepsilon_{\parallel}$ and $\varepsilon_{\perp}$ measured with the Aramis system and the in-plane stresses $\sigma_{\parallel}$ and $\sigma_{\perp}$ obtained from the laser induced delamination experiments.

Sample notation	Deformation (%)	$\varepsilon_{\parallel}$ (%)	$\varepsilon_{\perp}$ (%)	$\sigma_{\parallel}$ (MPa)	$\sigma_{\perp}$ (MPa)
p6s10m1	1.0	0.72 ± 0.06	-0.51 ± 0.04		
p4s10m5	1.0			5.9 ± 1.0	-3.0 ± 1.0
p4s10m2	1.0			5.6 ± 1.0	-3.1 ± 1.0
p6s15m1	1.5	1.15 ± 0.04	-0.64 ± 0.03		
	1.5				
p6s07m1	0.7	0.51 ± 0.03	-0.30 ± 0.03		
p4s07m1	0.7			5.6 ± 1.0	-3.1 ± 1.0
p4s07m2	0.7			3.5 ± 1.0	-2.2 ± 1.0

pending on the geometry of the experiment, delamination was studied under compressive or tensile in-plane stresses.

The presented model enabled us to recover from the experimental data not only the practical work of adhesion but also the magnitude and the character (tensile or compressive) of the in-plane stress. The in-plane stress obtained from the delamination measurements were compared to the strain fields directly measured on the metal substrate by optical methods.

ACKNOWLEDGMENTS

The authors would like to thank Emiel Amsterdam for the help in performing experiments with the Aramis system. This work was funded by the Netherlands Institute for Metals Research under Project No. MC7.05223.

[1]F. Deflorian, L. Fedrizzi, S. Rossi, Corros. Sci. **42**, 1283 (2000).
[2]L. F. Francis, A. V. McCormick, D. M. Vaessen, and J. A. Payne, J. Mater. Sci. **37**, 4717 (2002).
[3]Y. Yu, I. A. Ashcroft, and G. Swallowe, Int. J. Adhes. Adhes. **26**, 511 (2006).
[4]S. Guo, D. A. Dillard, and J. A. Nairn, Int. J. Adhes. Adhes. **26**, 285 (2006).
[5]H. M. Jensen and M. D. Thouless, Int. J. Solids Struct. **30**, 779 (1993).
[6]J. G. Williams, Int. J. Fract. **87**, 265 (1997).
[7]S. Guo, K.-T. Wan, and D. A. Dillard, Int. J. Solids Struct. **42**, 2771 (2005).
[8]J. Bouchet, A. A. Roche, and E. Jacquelin, J. Adhes. Sci. Technol. **15**, 345 (2001).
[9]H. R. Daghyani, L. Ye, and Y.-W. Mai, J. Mater. Sci. **31**, 2523 (1996).
[10]C. Gay, Int. J. Adhes. Adhes. **20** 387 (2000).
[11]R. Vayeda and J. Wang, Int. J. Adhes. Adhes. **27**, 480 (2007).
[12]C. S. Litteken, S. Strohband, and R. H. Dauskardt, Acta Mater. **53**, 1955 (2005).
[13]A. Fedorov and J. Th. M. De Hosson, J. Appl. Phys. **97**, 123510 (2005).
[14]A. Fedorov, R. van Tijum, W. P. Vellinga, and J. Th. M. De Hosson, J. Appl. Phys. **101**, 043520 (2007).
[15]B. Cotterell and Z. Chen, Int. J. Fract. **86**, 191 (1997).
[16]A. Fedorov, J. Th. M. De Hosson, R. van Tijum, and W. P. Vellinga, *Thin Films-Stresses and Mechanical Properties XI*, MRS Symposia Proceedings No. 875 (Materials Research Society, Pittsburgh, 2005), p. O4.19.
[17]S. P. Timoshenko and S. Woinowsky-Krieger, *Theory of Plates and Shells* (McGraw-Hill, 1959).
[18]A. V. Fedorov, R. van Tijum, W. P. Vellinga, and J. Th. M. De Hosson, Prog. Org. Coat. **58**, 180 (2007).
[19]W. H. Press, B. P. Flannery, S. A. Teukolsky, and W. T. Vetterling, *Numerical Recipes in Pascal* (Cambridge University Press, Cambridge, 1989).
[20]H. C. E. van der Aa, M. A. H. van der Aa, P. J. G. Schreurs, F. P. T. Baaijens, and W. J. van Veenen, Mech. Mater. **32**, 423 (2000).